

# How Do Layered Airspace Design Parameters Affect Airspace Capacity and Safety?

Prof.dr.ir. Jacco M. Hoekstra, Jerom Maas M.Sc.  
Martijn Tra B.Sc., Emmanuel Sunil, M.Sc.  
Faculty of Aerospace Engineering, TU Delft

**Abstract**—In many ATM studies experiments are performed to determine the capacity. This paper looks at the effect of airspace design on the capacity. Using an algebraic approach a relation is derived between the design parameters of a layered airspace design and the capacity of the airspace. The validity of the assumptions which are used in this derivation are tested experimentally. This airspace lay-out proved to be the airspace design which had the highest capacity for the unstructured, extremely high traffic demand used in an earlier experimental study. The result is both a method to relate an airspace design to the capacity as well as a relation which shows the effect on the airspace capacity for an airspace design where different levels or layers are defined each with their own segment of heading angles.

**Keywords** — *Capacity; Air Transportation System Performance Measurement; Traffic Complexity; Airspace Design; Conflict Probability; Conflict Rate; Separation Assurance; Safety*

## I. INTRODUCTION

Many studies aim to increase the capacity of Air Traffic Control (ATC) [1] [2], while others study the relation between traffic density and capacity [3] [4]. This paper is of the second category. Both types of studies acknowledge the strong relation between traffic conflicts and capacity, even though the exact, analytical relation is not known.

The ultimate goal of Air Traffic Control is to prevent aircraft from having collisions. Since the exact locations of aircraft are not known to Air Traffic Control, a safety buffer is used in the form of separation criteria. When two aircraft actually are closer to each other than specified in the defined separation criteria, this is called a *loss of separation*.

A *conflict*, on the other hand, is defined as a predicted, potential loss of separation within a specified prediction horizon, also called the look-ahead time. If a conflict is detected, it needs to be resolved to prevent the predicted loss of separation from actually happening, this is referred to as *conflict resolution*.

Maintaining separation can therefore be divided into two subtasks:

- conflict detection
- conflict resolution

Before the conflict detection & resolution (CD&R), there is a third option: prevent conflicts from happening. This is referred to as *conflict prevention*. This takes place before actual conflicts are detected. Air Traffic is organised in such a way that it lowers the chance of conflicts occurring. Airspace design is a way to prevent conflicts.

Other examples of conflict prevention are:

- Structuring of air traffic by an air traffic controller
- Using the semi-circular rule for headings and altitudes (eastbound at odd levels and westbound at even levels)
- Avoiding potential bottle-neck areas
- Limiting the number of aircraft entering an airspace

Conflict detection and resolution are tasks which are performed by humans and systems, both on the ground as well as in the air. Different task allocation combinations have become an important topic of ATM research as this might increase the airspace capacity or efficiency [5].

In this paper, the focus is on airspace design. If an airspace is designed in a way which lowers the potential number of conflicts, the amount of necessary conflict detections and resolutions decreases as well. In this way, the task load on the controller, pilot and the systems involved can be reduced. The number of conflicts per unit time is called the conflict rate and it is one of the main limiting factors for the capacity of an airspace.

Many attempts have been made to find geometrical metrics to define the capacity of the airspace via the task load considerations. When these metrics are aimed at measuring the load on human air traffic controllers, a metric like the so-called Dynamic Density [7], the traffic geometric complexity [8] or pragmatic variations of these [9] can be used.

However, as these definitions are very specific, or even require tuning, capacity limits found using these approaches are dependent of the level of automation, the task allocation and properties of the specific airspace considered.

Furthermore, future changes in automation or task allocation may change the metrics for the task load of resolving conflicts. However, these metrics will always be dependent on the conflict rate, and therefore on the design of the airspace. Hence, research on the effects of airspace design on conflict rate can lead to increases in airspace capacity.

In many projects, capacity limits are based mainly on conflict detection and resolution tasks, and are determined experimentally [4] [6]. An example which focusses on conflict prevention by airspace design for extreme traffic densities is the Metropolis project, where fast-time simulations consisting of millions of flights were performed to study the effect of airspace structure effects on capacity [10].

Next to experimental simulations, theoretical relations between airspace structure and the conflict rate are also needed. In this paper the effect of an airspace design is analysed by expressing, the conflict rate in terms of the design parameters of the airspace.

## II. THEORETICAL RELATIONS FOR GLOBAL CONFLICT RATE

The relationship between the global conflict rate for an airspace with the total number of aircraft  $N$  is described by [11][12]

$$CR_{global} = \binom{N}{2} p_2 \quad (1)$$

This relation can also be written as:

$$CR_{global} = \frac{1}{2} N(N-1) p_2 \quad (2)$$

With:

- $CR_{global}$  = global conflict rate in an airspace
- $N$  = total number of aircraft in an airspace
- $p_2$  = average conflict probability for any given pair of aircraft in this airspace

In words this relation (2) can be summarized as:

*The global conflict rate is equal to the number of possible combinations of two aircraft, multiplied with the conflict rate for any given pair.*

This equation can also be used to gain insight into the relation between capacity and safety. For example: the effect of decentralizing the task of separation assurance by moving it to the cockpit reduces the quadratic relation (2) to a linear relation when both aircraft are involved in solving a conflict:

$$CR_{local} = (N-1) p_2 \quad (3a)$$

In words:

*The local conflict rate is the number of other aircraft, multiplied with the general chance that any two aircraft meet each other in this specific airspace.*

The difference between the effect of traffic density on the centralised conflict rate on a global and decentralised level can be seen in Figure 1 [11].

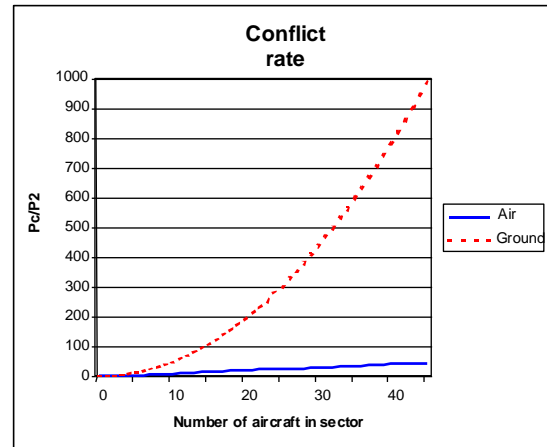


Figure 1 The relation between number of aircraft for centralized ('Ground') conflict rate and decentralized ('Air') conflict rate [11]

When using priority rules, a fail-safe is removed but the overall task load for humans and/or systems is halved, as only one of each pair of aircraft has to take action:

$$CR_{localpriority} = \frac{1}{2} (N-1) p_2 \quad (3b)$$

The same equation was later used by Jardin in [13] and [14] to derive  $p_2$  and study the effect of fixed routes versus free routing on the conflict rate. Jardin also added the effect of the average ground speed  $V$ , the lateral separation minimum  $R$  for the two-dimensional case (horizontal flight), the average time an aircraft spends in the airspace  $T_{FL}$  and the total airspace area  $A$  and observation time  $T_{tot}$ . This makes the conflict rate proportional to ratio of the area

‘swept’ by the aircraft and the total area of the airspace

$$CR_{global} \sim \frac{\bar{V} \cdot R \cdot T_{FL}}{A \cdot T_{tot}} \quad (4)$$

Imagine that all aircraft fly twice as fast, then the conflict rate will double as well, as the effect is similar to accelerating the time from a point of view of the pilot. Thus, the other aircraft then approach the ownship twice as fast. Consequently, the ground speeds affect the conflict rate via the relative velocity of the aircraft.

This example shows that the conflict rate is proportional to the relative velocity. As the doubling example illustrates, this relation also holds on a global level when we use the average relative velocity (at larger distances this is equal to the range rate for conflicting aircraft trajectories). Hence we can write:

$$CR_{global} \sim \bar{V}_{rel} \quad (5)$$

$$p_2 = c \cdot \bar{V}_{rel} \quad (6)$$

In which:

$\bar{V}_{rel}$  = relative velocity averaged over a/c pairs  
 $c$  = constant for a given airspace and number of aircraft

And effective airspace design performs conflict prevention by reducing the probability that two aircraft will have a conflict, in other words: it either lowers the  $p_2$ , or the  $V_{rel}$  in the above equations. The above equations form the starting point of the derivation in this paper.

### III. LAYERED AIRSPACE DESIGN AND CONFLICT PREVENTION

In the Metropolis project, the airspace capacity as a function of the level of structure in the airspace design has been investigated for extreme traffic densities. Scenarios were based on package delivering UAVs and personal air transport to overload an airspace to find capacity limits. In terms of safety the so-called Layers-airspace concept performed best [10] at a minimal cost in terms of efficiency.

This airspace concept used the airspace structure as depicted in Figure 2. Here, the airspace was divided in vertical segments, and to each layer a span of aircraft headings was assigned.

This means that the cruise altitude of an aircraft is dependent on the cruise heading. An exception was made for climbing and descending aircraft, allowing them to reach the level required for their preferred heading in an efficient way. For the climb and descent phases, a tactical conflict prevention, detection and resolution (CD&R) system was used.

What is the effect of this airspace design on conflict rate as expressed using the above equations? To answer this, two main effects which will be considered in this paper.

Safety Layer	6450 ft
Level Layer (315 to 360°)	6150 ft
Level Layer (270 to 315°)	5850 ft
Level Layer (225 to 270°)	5550 ft
Level Layer (180 to 225°)	5250 ft
Level Layer (135 to 180°)	4950 ft
Level Layer (90 to 135°)	4650 ft
Level Layer (45 to 90°)	4350 ft
Level Layer (0 to 45°)	4050 ft
Level Layer (315 to 360°)	3750 ft
Level Layer (270 to 315°)	3450 ft
Level Layer (225 to 270°)	3150 ft
Level Layer (180 to 225°)	2850 ft
Level Layer (135 to 180°)	2550 ft
Level Layer (90 to 135°)	2250 ft
Level Layer (45 to 90°)	1950 ft
Level Layer (0 to 45°)	1650 ft

Figure 2. Layers concept as used in the Metropolis project for UAVs and Personal Air Transport Vehicles

#### A. Spreading effect

The first effect is that separating the traffic over layers changes the combinations of aircraft pairs as we now have a vertical segmentation which separates the air traffic.

Imagine we defined L layers, and we assume that, on average, the traffic is evenly spread over the layers. This could be achieved by choosing the headings segments per layer wisely. In case of an uneven distribution of traffic over headings, more layers could be assigned to these directions, ensuring an

efficient use of airspace by evenly distributing the traffic over the layers.

For each layer we can then write the relation for conflict rate per layer:

$$CR_{layer} = \frac{1}{2} N_{layer} (N_{layer} - 1) p_{layer} \quad (7)$$

To compute the total expected conflict rate, a summation can be performed over multiple layers:

$$CR_{global} = \sum_{layer=1}^L \frac{1}{2} N_{layer} (N_{layer} - 1) p_{layer}$$

Equivalently, when it is assumed that aircraft are spread evenly over all flight levels and the conflict rate  $p_{layer}$  is equal in all layers:

$$CR_{global} = \frac{1}{2} N \left( \frac{N}{L} - 1 \right) p_2 \quad (8)$$

We can also see the effect of dividing the traffic over L layers by comparing this equation to Equation (2). Equation (2) can be seen as a special case for one layer, i.e. when  $L=1$ .

### B. Reduction of relative velocity effect

Next to spreading the traffic over different layers, the Layers design also uses heading segments per altitude band. More general we can call this angle, the heading span of a layer  $\alpha$  (alpha). In the example in Figure 2, the segment is 45 degrees or in other words:  $\alpha = \pi/4$ . As the 360 degrees ( $2\pi$ ) of all possible headings was evenly divided, 8 segments and two sets of 8 layers were used. The result is:  $L=16$  with  $\alpha = \pi/4$ .

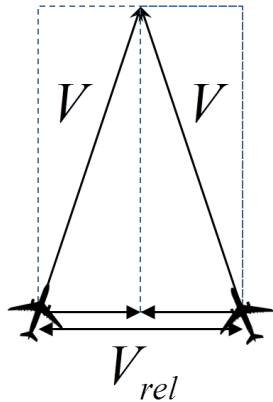


Figure 3. Geometric relation between heading difference for two aircraft with the same ground speed

This heading segment represents the maximum heading difference between two aircraft which could meet each other in a layer. To see the effect of heading difference, we consider two aircraft, both flying with the average ground speed. The relation between the relative velocity and the heading difference follows from the conflict geometry in Figure 3.

In reality the speeds will vary per aircraft combination, but when focussing on the global effect of heading difference by using the average ground speed  $V$ , the relative velocity can be expressed as a function of the heading difference:

$$V_{rel}(|\Delta hdg|) = 2V \sin\left(\frac{|\Delta hdg|}{2}\right) \quad (9)$$

In which:

$V_{rel}$  = Relative ground speed (scalar)

$V$  = Ground speed (scalar)

$|\Delta hdg|$  = Heading difference (absolute value of the difference of direction of two ground speed vectors)

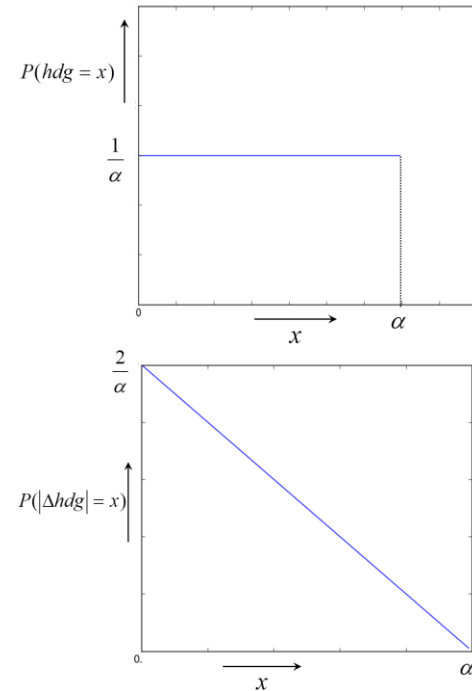


Figure 4: The absolute value of subtracting two uniform distribution results in a triangular distribution

Please note that in Equation (9) it is assumed that all aircraft fly with the same ground speed and the aircraft are flying towards the same point in time. Although the actual geometry can be very different when the aircraft miss each other at a large distance, those cases do not have to be included for the conflict rate. Two generalisations are made: identical, or similar, ground speed and the distance to the CPA is much larger than the separation criteria.

The average relative velocity within a single layer can be calculated based on the distribution of heading differences in that layer. Assuming a uniform distribution of the headings within a layer, the resulting probability density function for the heading difference becomes a triangular distribution as illustrated in Figure 4.

The resulting probability density function (pdf) for the heading difference is described by:

$$P(|\Delta hdg| = x) = \frac{2}{\alpha} \left(1 - \frac{x}{\alpha}\right) = \frac{2}{\alpha^2} (\alpha - x) \quad (10)$$

Using stochastic calculus, this distribution function for the heading difference can be used to calculate the average relative velocity. This is done by integrating the product of relative velocity as function of the heading difference with the probability distribution function for the relative heading using equation (9) and (10):

$$P_{layer} = c \cdot \bar{V}_{rel} \quad (11)$$

$$P_{layer} = \int_0^{\alpha} P(|\Delta hdg| = x) \cdot c \cdot V_{rel}(|\Delta hdg| = x) dx \quad (12)$$

$$P_{layer} = c \cdot \bar{V} \int_0^{\alpha} \frac{2}{\alpha^2} (\alpha - x) \sin \frac{x}{2} dx \quad (13)$$

$$P_{layer} = \frac{2c\bar{V}}{\alpha^2} \int_0^{\alpha} (\alpha - x) \sin \frac{x}{2} dx \quad (14)$$

$$P_{layer} = \frac{2c\bar{V}}{\alpha^2} \left( \int_0^{\alpha} \alpha \sin \frac{x}{2} dx - \int_0^{\alpha} x \sin \frac{x}{2} dx \right) \quad (15)$$

$$P_{layer} = \frac{2c\bar{V}}{\alpha^2} \left( \left[ -2\alpha \cos \frac{x}{2} \right]_0^{\alpha} - \left[ -2x \cos \frac{x}{2} + 4 \sin \frac{x}{2} \right]_0^{\alpha} \right) \quad (16)$$

$$P_{layer} = \frac{4c\bar{V}}{\alpha^2} \left( \left( -\alpha \cos \frac{\alpha}{2} + \alpha \right) - \left( -\alpha \cos \frac{\alpha}{2} + 2 \sin \frac{\alpha}{2} \right) \right) \quad (17)$$

$$P_{layer} = \frac{4c\bar{V}}{\alpha^2} \left( \alpha - 2 \sin \frac{\alpha}{2} \right) \quad (18)$$

$$P_{layer} = \frac{4c\bar{V}}{\alpha} \left( 1 - \frac{2}{\alpha} \sin \frac{\alpha}{2} \right) \quad (19)$$

$$P_{layer} = 4c\bar{V} \cdot \frac{1}{\alpha} \left( 1 - \frac{2}{\alpha} \sin \frac{\alpha}{2} \right) \quad (20)$$

Since the main goal of this derivation is to analyse the effect of the heading segment  $\alpha$ , we move the other aspects to a constant  $k$  for now.

$$P_{layer} = k \cdot \frac{1}{\alpha} \left( 1 - \frac{2}{\alpha} \sin \frac{\alpha}{2} \right) \quad (21)$$

#### IV. COMBINING THE SPREADING EFFECT AND RELATIVE VELOCITY EFFECT

Combining the equation (8) and (20) gives the total effect of the airspace structure for  $N$  aircraft with  $L$  layers based on reducing the heading segments  $\alpha$ .

$$CR_{global} = \frac{1}{2} N \left( \frac{N}{L} - 1 \right) \cdot \frac{1}{\alpha} \left( 1 - \frac{2}{\alpha} \sin \frac{\alpha}{2} \right) \cdot k \quad (22)$$

This equation shows the distinct influence of the two beneficial effects of a layered airspace structure based on heading segments.

$$CR_{global} = \underbrace{\frac{1}{2} N \left( \frac{N}{L} - 1 \right)}_{\text{spreading effect}} \cdot \underbrace{\frac{1}{\alpha} \left( 1 - \frac{2}{\alpha} \sin \frac{\alpha}{2} \right)}_{\text{reduced relative velocity effect}} \cdot \underbrace{k}_{\text{other influences}} \quad (22)$$

This equation can also be used when no restrictions on heading are applied, substituting  $L=1$  and  $\alpha=2\pi$ , in which case it returns to the form similar to that of Equation (8):

$$CR_{global} = \frac{1}{2} N(N-1) \cdot \frac{k}{2\pi} \quad (23)$$

Combining this equation with Equation (22) given the relation between the conflict rate with layers and the conflict rate without the layers:

$$[CR_{global}]_L = [CR_{global}]_{L=1} \cdot \underbrace{\frac{N-L}{L(N-1)}}_{\text{spreading factor}} \cdot \underbrace{\frac{2\pi}{\alpha} \left( 1 - \frac{2}{\alpha} \sin \frac{\alpha}{2} \right)}_{\text{heading segment factor}} \quad (24)$$

The effect of the semi-circular rule can now be expressed in factors as well, when compared to aircraft with all possible headings flying at the same altitude. Assume an airspace with 100 aircraft, and 10 segments: 5 for eastbound traffic and 5 for westbound traffic. Equation 25 then shows the effect of using this rule, as  $N=100$ ,  $L=10$  and  $\alpha=\pi$ :

$$\begin{aligned} [CR_{global}]_L &= [CR_{global}]_{L=1} \cdot \underbrace{\frac{100-10}{10 \cdot 99}}_{\text{spreading factor}} \cdot \underbrace{\frac{2\pi}{\pi} \left(1 - \frac{2}{\pi} \sin \frac{\pi}{2}\right)}_{\text{heading segment factor}} \\ &= [CR_{global}]_{L=1} \cdot 0.09 \cdot 0.73 \quad (25) \end{aligned}$$

This shows that in this example, using the semi-circular rule reduces the conflict rate with a factor of 15. It also shows that splitting the airspace into 10 layers has the largest effect (91% reduction), while using only two heading segments results in a reduction of 27%.

The table below shows the heading effect for a number of heading segment sizes:

Table 1. Heading segment effect on conflict rate

alpha (deg)	Conflict reduction
360	0%
180	27%
90	60%
45	80%
22.5	90%
10	95%

Assuming there is a maximum allowable conflict rate, equation (22) can also be used to determine the capacity:

$$\begin{aligned} CR_{global} &= k \frac{1}{2} N \left( \frac{N}{L} - 1 \right) f(\alpha) \\ \text{with } f(\alpha) &= \frac{1}{\alpha} \left( 1 - \frac{2}{\alpha} \sin \frac{\alpha}{2} \right) \quad (26) \end{aligned}$$

We can use equation (26) to determine the capacity:

$$CR_{max} = \frac{1}{2} k f(\alpha) \left( \frac{N^2}{L} - N \right) \quad (27)$$

$$\frac{1}{L} N^2 - N - \frac{2 \cdot CR_{max}}{k f(\alpha)} = 0 \quad (28)$$

Solving this yields:

$$\begin{aligned} N_{max} &= \frac{1}{2} L + \frac{1}{2} \sqrt{L^2 + \frac{8L CR_{max}}{k f(\alpha)}} \\ \text{with } f(\alpha) &= \frac{1}{\alpha} \left( 1 - \frac{2}{\alpha} \sin \frac{\alpha}{2} \right) \quad (29) \end{aligned}$$

Finally, Equation (26) can also be combined with the Equation (4) to incorporate the ratio between the area searched for conflicts and the total area of the airspace. In this way, all relevant airspace design parameters have been considered:

$$\begin{aligned} CR_{global} &= k \cdot \frac{\bar{V} R T_{FL}}{A T_{tot}} \frac{1}{2} N \left( \frac{N}{L} - 1 \right) f(\alpha) \\ \text{with } f(\alpha) &= \frac{1}{\alpha} \left( 1 - \frac{2}{\alpha} \sin \frac{\alpha}{2} \right) \quad (30) \end{aligned}$$

With:

$k^*$  = constant

$\bar{V}$  = average ground speed

$T_{FL}$  = average time spent in airspace

$T_{tot}$  = total time span

$A$  = area of airspace

$N$  = total number of aircraft

$L$  = number of subdivisions (layers)

$\alpha$  = heading range per subdivision of airspace

When no heading segments are used, the value of  $\alpha$  is 360 degrees, making  $f(\alpha)$  equal to  $1/2\pi$  (the  $2\pi$  is accounted for in the constant  $k$ ). Any equal subdivision of airspace can be expressed in terms of the number of layers  $L$ .

A number of assumptions were made along the way in the derivation. They are summarized below:

1. The conflict probability of two aircraft is proportional to their relative velocity
2. The ground speed of each aircraft is equal
3. The aircraft do not make turns

## V. VALIDATION

To test the validity of equation (30) a number of simulations were run. In these simulations, the focus is on the function  $f(a)$ . The independent variable was thus the heading span  $a$  of the simulated layer.

In each simulation an airspace was formed and aircraft were created in this airspace. After the

random initial condition, conflicts are counted within the look-ahead time. After each count, the next iteration was started. The experiment parameters are given in table 2.

Number of aircraft:	150
Initial aircraft position:	Random (uniform) in creation region
Creation region size:	1500 nm x 1500 nm
Ground speed :	400 kts
Heading:	Random (uniform) in heading span $[0, a]$
Protected zone radius:	5 nm
Number of simulations:	10000 - 100000

Table 2: Experiment parameters

As the goal is to analyse how many conflict arise per time unit, initial intrusions are avoided in the start condition as a zero relative speed should correspond with a conflict rate of zero.

The remaining constant  $k$  in the relation (30) is independent of  $a$ . In order to compare the theoretical and experimental conflict rates, it is assigned a scalar value. The value of  $k$  is used as a scaling parameter.

In the following figures, both the theoretical and experimental relations are plotted next to each other. The blue line is the theoretical relation between the dependent and independent variables. The red dots show a scatter plot, where each simulation is represented as one point. The scatter plots contain 10,000 points, as 10,000 different simulations were performed.

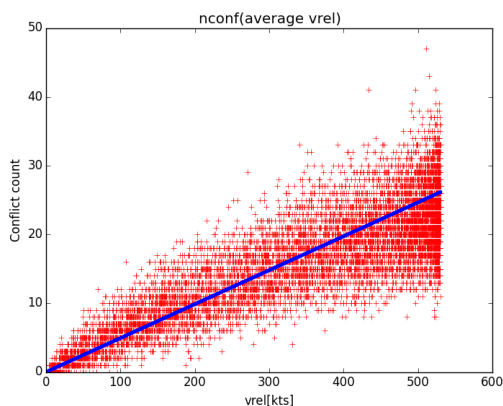


Figure 5: Experimental and theoretical relations between  $V_{rel}$  and conflict count

First the average relative velocity is plotted against the conflict rate. This tests the relation between the average relative velocity magnitude in one simulation, and the number of conflicts. The

theoretical line follows hypothesis 1: this relation is assumed to be linear. The results can be seen in Figure 5.

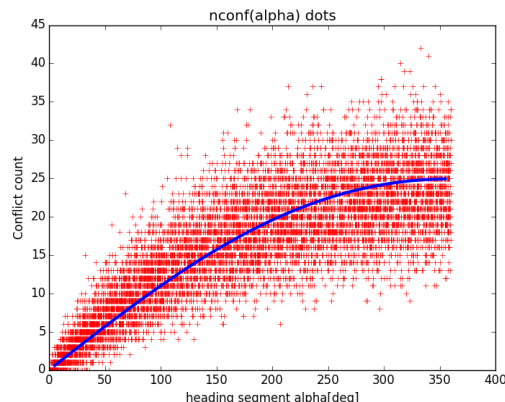


Figure 6: Experimental (red) and theoretical (blue) relations between heading span and conflict count.

It is found that this relation does indeed follow the expected pattern: the conflict count is proportional to  $V_{rel}$ . Next, the effect conflict relation (30) is tested. Now, the  $V_{rel}$  is not given on the x-axis, but the heading span  $a$  of the layer. The result is seen in Figure 6. The experimental data in the scatter plot are sorted in bins of 10 degrees heading span width. Of each bin the average conflict count is computed, and the result is a line, indicated in figure 7. Here it can be seen that the theoretical prediction of conflict count (Equation 30) closely matches the experimental simulation results

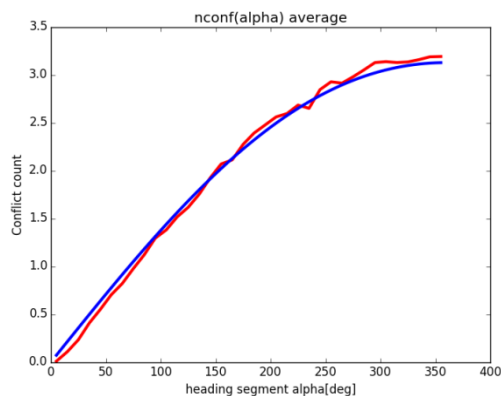


Figure 7: Averaging the data points from only several experiment runs allows to compare the experimental (red) and theoretical (blue) relations for heading span per layer and conflict count

## VI. CONCLUSIONS

The conflict rate in an airspace is proportional to the conflict probability and hence it is an indication for

safety. The conflict rate is, in turn, proportional to the relative velocity.

Using the conflict probability model for direct routing airspace from [11] as a starting point, a relation that connects the conflict rate with the design parameters of a layered airspace concept has been found. This function has been derived using the equations for 2D conflict geometry, probability distributions and the assumptions that aircraft fly straight paths with constant velocities.

For  $L$  layers, each with a heading segment of  $\alpha$  degrees, the conflict rate can be expressed as:

$$CR_{global} = \frac{1}{2} N \left( \frac{N}{L} - 1 \right) \cdot \frac{1}{\alpha} \left( 1 - \frac{2}{\alpha} \sin \frac{\alpha}{2} \right) \cdot \frac{\bar{V} R T_{FL}}{A T_{tot}} \cdot k$$

In this equation the symbols have the following meaning:

- $L$  : number of layers
- $N$  : global number of aircraft
- $\alpha$  : heading span of a layer
- $V$  : average ground speed of aircraft
- $R$  : horizontal separation requirement
- $T_{FL}$  : time spent in airspace
- $T_{tot}$  : total observation/experiment time span
- $A$  : area of the airspace
- $k$  : constant for airspace structure aspects

The equation consists of three distinct elements. In the first factor, the conflict rate is reduced as a consequence of spreading the traffic over multiple layers. The second factor is a reduction of conflict rate due to the sorting of aircraft in each layer by heading. Combining this with the results by Jardin [14] results in an additional, third, factor, which accounts for other effects such as the size, the traffic ground speed and structure of the airspace.

A validation was performed by computer simulations, which show strong correlations between theoretical and experimental results.

Future research can build on this work by further expanding or detailing this relation. For instance, additional dependencies on the model constant  $k$ , such different variations in the ground speeds and including the effect of descending and climbing traffic through cruise layers.

The given relation, can be used for vertical segmentations of airspaces. The followed method of using the distributions of relative velocities and

heading differences analytically is more widely applicable. It is also an addition to the many empirical traffic complexity weighing factors which is more fundamental, The method presented here for one type of airspace design, can be used to relate many other, more conventional, airspace design parameters, air traffic complexity and capacity to each other in many different ways. Future research can use this relative speed and relative heading effect method to find similar relations, both generic and geo-specific for a variety of airspaces..

## REFERENCES

- [1] R. Irvine, "Investigating the capacity benefit of airborne speed adjustment", FAA/Eurocontrol ATM Seminar 2015, Lissabon, 2015
- [2] S. Ruiz, M.Soler, "Conflict pattern analysis under the consideration of optimal trajectories in the European ATM", FAA/Eurocontrol ATM Seminar 2015, Lissabon, 2015
- [3] P. Brooker, "Control Workload, Airspace Capacity and Future Systems", Human Factors and Aerospace Safety 3(1), 2003
- [4] G. Tobaruela, A. Majumbar, W.Y. Ochieng, "Identifying Airspace Capacity Factors in the Air Traffic Management System", ATACCS'2012, London, 2012
- [5] M. IJtsma, J.M.Hoekstra, R. Bhattacharyya, A. Pritchett "Computational Assessment of Different Air-Ground Allocations", 11<sup>th</sup> FAA/Eurocontrol ATM Seminar, Lissabon, 2015
- [6] K.J.Leiden, P.Kopardekar, S. Green, "Controller Workload Analysis Methodology to Predict Increases in Airspace Capacity", AIAA 3<sup>rd</sup> ATIO Tech 2003, Denver, 2003
- [7] P. Kopardekar, A. Schwarz, S. Magyarits, J. Rhodes, "Airspace Complexity Measurement: An Air Traffic Control Simulation Analysis", International Journal of Industrial Engineering, 16(1), 2009
- [8] D. Delahaye, S. Puechmorel, "Air Traffic Complexity: Towards Intrinsic Metrics", 3<sup>rd</sup>, FAA/Eurocontrol ATM Seminar, Napoli, 2000
- [9] G.M. Flynn, C. Leleu, B. Hilburn, "A Complexity Study of the Maastricht Upper Airspace Centre", EEC Report No. 403, Project COCA, Eurocontrol Experiment Centre, Brétigny, 2006
- [10] E. Sunil, J.M.Hoekstra, J. Ellerbroek, et al, "Metropolis: Relating Airspace Structure and Capacity for Extreme Traffic Densities", 11<sup>th</sup> FAA/Eurocontrol ATM Seminar, Lissabon, 2015[13]
- [11] J.M. Hoekstra, R.C.J. Ruigrok, R.N.H.W. van Gent, "Free Flight in Crowded Airspace?", 3<sup>rd</sup> FAA/Eurocontrol ATM Seminar, Napoli, 2000
- [12] J.M. Hoekstra, "Designing for Safety: Free Flight with Airborne Separation Assurance", Doctoral Thesis, TU Delft, Delft, 2001
- [13] M.R. Jardin, "Air Traffic Conflict Models", AIAA ATIO forum, Chicago, 2004
- [14] M.R. Jardin, "Analytical relationships between Conflict Counts and Air Traffic Density", Journal of Guidance, Control and Dynamics, Vol. 28, No.6, 2005